Pure & Appl. Chem., Vol. 62, No. 5, pp. 803–814, 1990.
Printed in Great Britain.

The mathematical modelling of premixed turbulent combustion

Derek Bradley and A.K.C. Lau

Mechanical Engineering Department, Leeds University, Leeds LS2 9JT, U.K.

Abstract - The laminar flamelet approach to the modelling of turbulent combustion, based upon detailed chemical kinetics, is described. Allowance must be made for the effects of flame straining and the relationship between this in laminar and turbulent flames is discussed. Finally, some examples are given of computed combustion fields.

INTRODUCTION

Since the presentation of an earlier review in 1983 at a Workshop of the Siberian Academy of Sciences (ref. 1) there has been significant progress in the mathematical modelling of premixed turbulent combustion. Detailed chemistry has been incorporated through the concept of laminar flames in a turbulent fluid, and measurements in various systems have advanced our understanding of this complex phenomenon. There are, however, still a number of unresolved problems, not least those connected with the effects of flame straining. The present paper reviews some of these important issues. Régimes of turbulent flames are first discussed, to be followed by a review of flow field modelling and the unstrained flamelet model for turbulent combustion. The concept of strained flamelets in turbulence and a preliminary strained flamelet model are introduced and applied to recirculating combustion.

REGIMES OF TURBULENT COMBUSTION

Important parameters in the description of premixed turbulent flames are r.m.s. turbulent velocity, u', the unstrained laminar burning velocity, u_l, the integral length scale, L, and the laminar flame thickness, δ_l. The Borghi diagram with u'/u_l and L/δ_l as axes conveniently expresses the régimes of turbulent combustion (ref. 2). Abdel-Gayed et al have shown that, for isotropic turbulence, straight lines of constant Karlovitz stretch factor, K, $(=(u'/\lambda)(\delta_l/u_l))$ and of constant turbulent Reynolds number, R_L, $(= u'L/\nu)$ also can be shown on the diagram and these delineate different régimes (ref. 3). Here, λ is the Taylor microscale and ν the kinematic viscosity. For homogeneous and isotropic turbulence, with $\delta_l = \nu/u_l$ it is shown in ref. 4 that

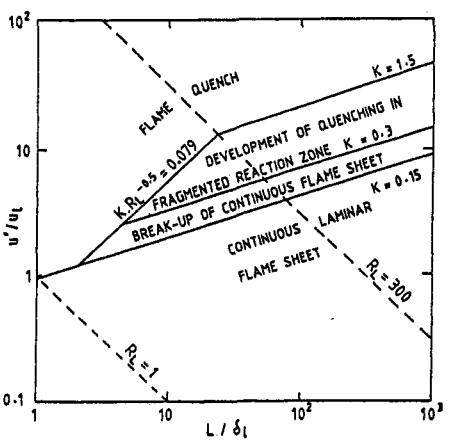

$$K = 0.157 \left(\frac{u'}{u_l}\right)^2 R_L^{-0.5} \qquad (1)$$

Fig. 1. Turbulent flame régimes.

All turbulent parameters and λ refer to the cold premixture. The different régimes, based upon experimental observations of explosion flames, are indicated in Fig 1, from ref. 3, for Lewis numbers close to unity. A continuous laminar flame sheet breaks up when values of K are increased to between 0.15 and 0.3. The chemical time, δ_l/u_l,

becomes greater than the Kolmogorov time when K attains a value of 0.258. Between these limits the break-up of the sheet is followed by localised quenching of some flamelets in a fragmented reaction zone, until, at higher values of K, the flame is completely quenched.

The eulerian strain rate, taken as u'/λ, is a mean value, as must be that of K. In practice, there is a distribution of different values and the described regimes are statistical in nature. For example, the values of K for the onset of flame quenching in Fig. 1 (e.g. K = 1.5 for $R_L > 300$) were defined by experimental ignitions with an 80% probability of successful flame propagation for a minimum of 20 spark ignitions (ref. 5).

Different criteria have been proposed for the limits of wrinkled laminar flame, often called flamelet, concepts (ref. 6). A particularly common one is that the laminar flame thickness should be less than the Kolmogorov microscale (ref. 7). This leads to (ref. 6)

$$\frac{u'}{u_l} < 1.281\ R_L^{0.25} \qquad (2)$$

With Eq (1) this is equivalent to $K < 0.258$. When K attains this numerical value the chemical and Kolmogorov lifetimes are equal. In this approach, however, it must be remembered that such quantification is, of necessity, simplified and that, in practice, there is a distribution of values of the strain rate.

Although Fig. 1 is a good guide to the nature of turbulent flames propagating into unburnt isotropic premixture of known physico-chemical characteristics, care must be taken over its application to other conditions. For example, the recirculation of hot gases into unburnt mixture, as employed in industrial furnaces and gas turbine combustion chambers to enhance stability, creates a different flame brush structure and can make definitions of flame front and burning velocity difficult, if not impossible. It will be shown later that combustion can occur in recirculating flows even when there are regions where the values of K are so high that Fig. 1 suggests flame quenching.

MODELLING OF THE FLOW FIELD

The spatially-varying flow and reaction fields in most practical combustors necessitate complex computational approaches. Transport statistical type models such as the k-ε and direct stress models have been employed to obtain global fields (refs. 8-11). In these models, various statistical mean turbulent quantities are computed from their modelled transport equations, but information on the dynamic behaviour of turbulence is, inevitably, truncated and irrecoverable. A transport dynamic model, in which some kind of transport equations govern the dynamic behaviour of the turbulence, has yet to be established. Direct simulation of the Navier-Stokes equation and recent developments in fractal dynamics and chaos theory might provide alternatives to the current transport statistical models which nevertheless, in many cases, provide adequate engineering solutions.

In isothermal elliptic turbulent flows it has been shown that the higher order direct stress, rather than the lower order k-ε, turbulence model is superior for flows with strong streamline curvature and anisotropic Reynolds stresses, such as occur, in particular, with secondary recirculation (refs. 10-12). The k-ε model over-attenuates swirling velocities with axial distance (ref. 13). When combustion occurs, the problems increase and the direct stress model is incomplete, with a number of controversial issues still to be resolved (refs. 14,15). These include, for example, the role of pressure fluctuations with changing density and their relation to flame-generated turbulence (refs. 16,17). Also, because of the computational complexity of a large number of coupled governing equations, solution is a formidable task in multi-dimensional flows, although recently some preliminary results have been obtained by the present authors and coworkers for two-dimensional premixed swirling and non-swirling flames in cylindrical burners. These show that with the flame located along a shear layer, the direct stress and k-ε model solutions of the temperature fields are only marginally different.

The nature of the numerical methods employed to solve the nonlinear set of coupled equations is most important. With a lower order numerical discretization scheme for the convection term in the governing equation, numerical errors can arise, to give results that do not reflect the true solution of the physical model (refs. 10-12, 18,19). Higher order numerical schemes are potentially more accurate but are usually associated with unboundedness characteristics. Consequently, there might be undesired oscillations, with

over and under-shoots in the solution. To overcome such effects, a higher order boundedness-preserving scheme, with the acronym SMART (Sharp and Monotonic Algorithm for Realistic Transport), has recently been developed at Leeds to solve the governing equations (ref. 20).

FLAMELET CONCEPTS OF TURBULENT COMBUSTION

To model the chemical reaction rates in the transport equations for each chemical species and for energy in turbulent combusting flow is a formidable task. The use of global reaction rates in turbulent combustion computation gave only limited success (ref. 21) and was superseded at Leeds by a laminar flamelet concept of turbulent combustion, with a detailed chemical kinetic laminar flame submodel (refs. 22,23). Because flames propagate through the agency of such rapid molecular phenomena as diffusion, conduction and chemical reaction, a turbulent flame might be regarded instantaneously as an array of flamelets in which molecular phenomena dominate. With laminar flamelets of the same structure as laminar flames of the same premixture, the computer-based modelling of turbulent combustion is much facilitated. Laminar flame structure is computed in a laminar flame sub-model with a full chemical kinetic scheme and profiles, such as those of species reaction rates and volumetric heat release rate, are expressed in terms of a single reaction progress variable.

In this approach the reaction progress variable, or reactedness, θ, is the dimensionless temperature rise, $(T-T_u)/(T_b-T_u)$ where T is the gas temperature and the subscripts "u" and "b" indicate unburnt and burnt gas conditions, respectively. For each particular temperature, there is a corresponding, single valued, volumetric heat release rate which is taken to be the same as that in a laminar flame of the same premixture, q_l.

Turbulence gives rise to temporal variations in the heat release rate, q, taken to be the same as q_l. There must be a probability density function (pdf) of q, namely p(q), and with the modelled assumption of its equality to that of θ, namely $p(\theta)$, the mean, mass weighted, volumetric heat release rate in the turbulent flame is

$$\tilde{q}_t = \int_0^1 qp(q)dq = \int_0^1 q_l(\theta)p(\theta)d\theta \qquad (3)$$

In subsequent figures values of $\tilde{q}_t$ will be normalised by the maximum value attained in the laminar flame, $q_{l\max}$. Throughout, ~, indicates a mass weighted average.

The considerations of the previous section suggest the use of a single reaction progress variable and laminar flame submodel might become invalid when the flame sheet is disrupted by flame stretch at a value of K of about 0.258, or greater. However, the regime of validity would be greater than this if a locally fragmented flame sheet reformed to give a relationship between reaction rate and θ that is not too dissimilar from that in the laminar flame. On the other hand, if for such values of K all reactions were to be quenched completely, the validity of the submodel automatically would be assured. If, as seems likely, a flame strain rate does not significantly change during reaction, the statistical distribution of strain rates would ensure that some flamelets maintained the combustion, whilst higher strain rates would abort some potential flamelets.

The present level of both understanding and computer power necessitates an 'a priori' assumption about the form of $p(\theta)$. In the Bray, Moss and Libby model, the pdf is dominated by values at $\theta = 0$ and $\theta = 1$: at any point in the turbulent flame the gases are either completely unburnt or burnt (ref. 24). The validity of this assumption increases as the flame thickness tends to zero and the chemical reaction rate to infinity, namely, at high values of R_L and low values of K (high Damköhler number), as shown in Fig. 1. Then the two delta functions for unburnt and burnt gas that comprise $p(\theta)$ are related to the first moment of θ, which becomes a prime dependent variable. Such functions in Eq (3) would give no heat release and, as an alternative, the reaction rate at a point is expressed in terms of a flamelet crossing frequency. Recent work (ref. 25) suggests this frequency depends upon the time autocorrelation of $p(\theta)$ and a related integral timescale and that these can be generated experimentally (ref. 26).

The approach of Bradley et al in refs. 10 and 23 eschews assumptions of small flame thickness and infinite reaction rates by departing from the two delta functions at $\theta = 0$ and 1, to employ a beta function for $p(\theta)$ based upon first and second moment modelling of θ. These moments are obtained from the energy equation, but closure of this at the third moment level is not presently possible with sufficient accuracy. Although the beta

function is of flexible shape and can express bimodality, it cannot attain singular peak values at $\theta = 0$ and 1. More appropriate pdfs are a possibility, but knowledge of the required form is hindered by a dearth of accurate experimental data.

As with the mean volumetric heat release rate in a turbulent flame, a mean, mass weighted, species concentration can be expressed in terms of the species concentration in the laminar flame, $m_l(\theta)$ by

$$\tilde{m}_t = \int_0^1 m_l(\theta)p(\theta)d\theta \qquad (4)$$

The energy equation for the second moment of θ requires the evaluation of the covariance of the fluctuating progress variable and heat release rate, $\widetilde{\theta'q'}$ (ref. 23). This is given by

$$\widetilde{\theta'q'} = \int_0^1 (\theta-\tilde{\theta})q_l(\theta)p(\theta)d\theta \qquad (5)$$

The convenience of this flamelet approach is that detailed laminar profiles, such as $q_l(\theta)$ and $m_l(\theta)$, can be computed separately from detailed chemical kinetics and subsequently implemented in turbulent combustion computations through Eqs (3)-(5). Figures 2(a) and (b) show the contours of the normalised integrals of Eqs (3) and (5) for a turbulent methane-air premixture of equivalence ratio, ϕ, of 0.63, in terms of the mean value of θ, and the square root of its variant, g. Here $p(\theta)$ is a beta function, defined by the first two moments of θ. The pressure and initial temperature are atmospheric. The q_l profile is that computed by Dixon-Lewis (ref. 27) for an unstrained flame with detailed kinetics. The value of $q_{l_{max}}$ is 0.63 GW m^{-3}. For $g = 0$, the contour values in Fig. 2(a) corresponds to those of the laminar flame and $\widetilde{\theta'q'} = 0$. With infinitely fast chemistry, composition at a point in the turbulent flame brush fluctuates between wholly burnt products or wholly unburnt premixture. This condition is given by the semicircular envelope of normalised heat release rate in Fig. 2 with $g = [\tilde{\theta}(1-\tilde{\theta})]^{0.5}$ (ref. 28) and both $\tilde{q}_t$ and $\widetilde{\theta'q'}$ identically zero.

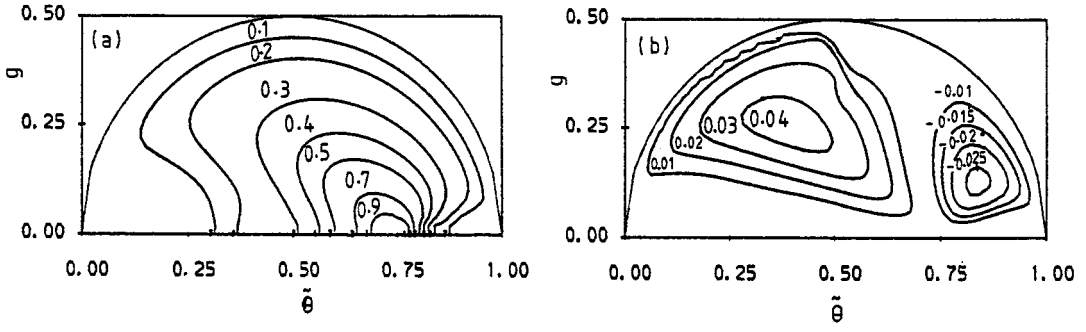

Fig. 2. Methane-air, $\phi = 0.63$. Contours of
(a) $\tilde{q}_t/q_{l_{max}}$ (b) $\widetilde{\theta'q'}/q_{l_{max}}$

STRAINED LAMINAR FLAMES

Classical theories of laminar premixed flames have assumed that both the flame and the associated flow are one-dimensional. In practice, there is some sideways flow arising from the pressure drop across the flame. This introduces, however slightly, a degree of flame straining. By virtue of this extra component of convective flow, which can be deliberately and appreciably increased, the balance between axial convection, conductive and diffusive energy fluxes is changed. If A is the area of a material surface element normal to the flow into the flame and t is the time, the strain rate is $(A)^{-1}dA/dt$. Furthermore, this is the maximum strain rate in any plane. It was shown theoretically, some time ago, by Klimov in ref. 29 that straining of such a flame can reduce the burning velocity, ultimately to extinction and this has subsequently been demonstrated experimentally in refs. 30 and 31. Asymptotic mathematical analyses reveal that Karlovitz stretch factor, as well as flame curvature, Lewis and Zeldovich numbers are all relevant to the phenomenon (ref. 32).

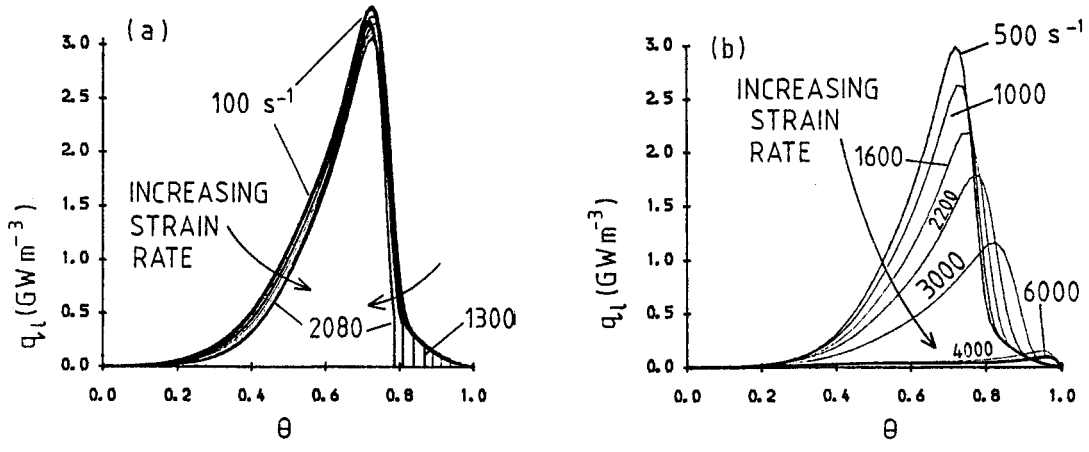

Fig. 3. Heat release rate - reactedness profiles, methane-air, ϕ = 0.84. (a) Symmetric flow, 11 strain rates. (b) Asymmetric flow, 8 strain rates.

More precise detailed laminar flame structures are currently being computed for different strain rates from mathematical models with detailed chemical kinetics (refs. 33,34). Shown in Fig. 3(a) are volumetric heat release rate-reactedness profiles obtained in this way by Dixon-Lewis and Missaghi for a methane-air mixture of equivalence ratio 0.84, with initially atmospheric conditions in eleven flames and with different, constant, strain rates, ranging from 100 to 2080 s^{-1} (ref. 35). The strain rates were achieved in parallel, but counterflowing, streams. In the symmetric case, shown here, both flows were initially of the cold premixture which reacted in the central region. Up to the flame quenching strain rate, there is little effect of strain rate upon the profile. In the asymmetric case one stream was of the cold premixture, the other was of the equilibrated products of combustion at the adiabatic temperature. In this case, shown in Fig. 3(b), rather different profiles were obtained at the different strain rates.

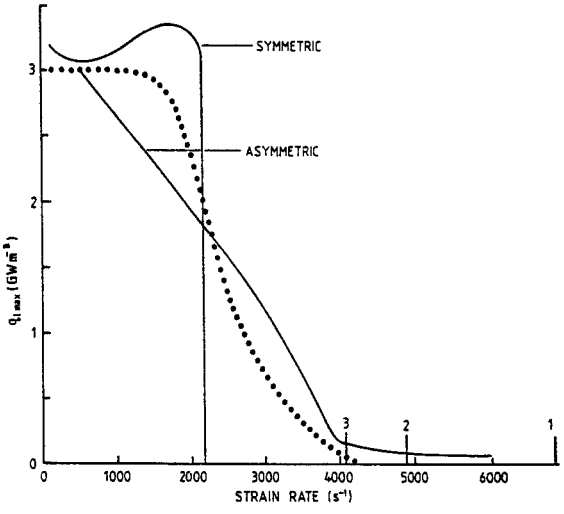

Fig. 4. Methane-air, ϕ = 0.84, changes in maximum heat release rate with strain rate.

Shown in Fig. 4 are the computed changes in the maximum values of the laminar flame heat release rates, $q_{l\,max}$, with strain rate. For the symmetric case, again the heat release rate does not change significantly with strain rate, although the maximum temperature is reduced below the adiabatic value. However, the flame extinguishes abruptly at a quenching rate of about 2,200 s^{-1}. The asymmetric case is different in that there is an approximately linear decrease of heat release with strain rate. The flame is maintained by the hot gases of the counterstream and, theoretically, never extinguishes completely, although it does in practice. Clearly, the heat release rate depends not only upon the magnitude of the strain rate, but also upon the geometric details of the straining process.

TURBULENT COMBUSTION COMPUTATIONS

Figure 5 parallels Fig. 2, but for ϕ = 0.84, and shows, for the symmetric counterflow condition, not surprisingly, the relatively small computed effect of given strain rates that are less than the quenching limit, upon the turbulent mean volumetric heat release

rate and covariance, $\widetilde{\theta' q'}$. Again a beta function was assumed for the reaction progress variable fluctuations and applied to the same conditions as Fig. 3(a). Only normalised contours for heat release rate and covariance values of 0.2 and 0.02, respectively, are shown. These are for constant, single-valued, strain rates of 100, 1100 and 2080 sec^{-1}. For this mixture the value of q_{1max} is 4 GW m^{-3}. The differences due to strain rate are probably within the uncertainty limits of other factors, not least the assumed beta function for the pdf of the dimensionless temperature rise reaction progress variable, θ. Clearly, a rectangular profile of heat release rate against flame strain rate, with a sharp cut-off and sudden quenching value of the latter, would be computationally advantageous.

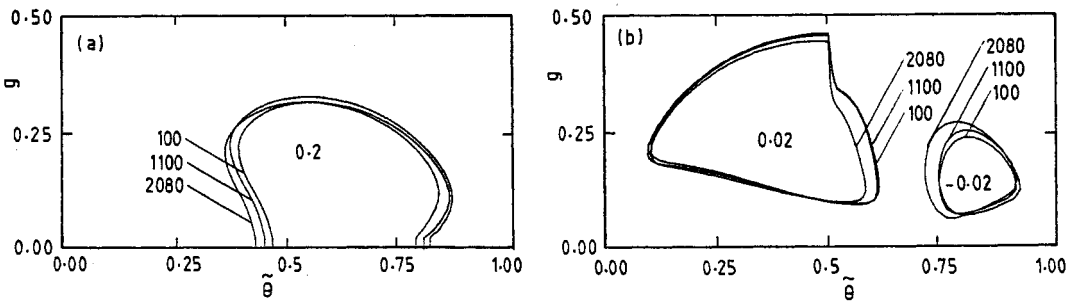

Fig. 5. Methane - air, $\phi = 0.84$. Effect of three strain rates (s^{-1}) in symmetric flow on the 0.2 and 0.02 contours of
(a) $\tilde{q}_t/q_{1max}$ (b) $\widetilde{\theta' q'}/q_{1max}$

Formalistically, Eq (3) might be extended to express the influence of strain rate and its distribution upon the mean turbulent heat release rate, as follows

$$\tilde{q}_t = \int_{-\infty}^{\infty} \int_{0}^{1} q_1(s,\theta)\ p(s,\theta)\ d\theta\ ds \qquad (6)$$

In this case the laminar heat release rate $q_1(s,\theta)$ depends upon the strain rate, s, as well as upon the reaction progress variable, and $p(s,\theta)$ is the joint pdf of s and θ. As there is no currently foreseeable means of accurately evaluating $p(s,\theta)$, it is computationally attractive if we assume, not unreasonably at this stage, that strain rates are uncorrelated with θ and the joint pdf is the product of the separated pdfs, $p(s)$ and $p(\theta)$. If we further assume that the laminar heat release rate is unaffected by strain until a limit quenching strain rate, S_q, is attained, above which value no heat release occurs and that all strain rates are positive, then Eq (6) becomes

$$\tilde{q}_t = \int_{0}^{S_q} p(s)ds \int_{0}^{1} q_1(\theta)p(\theta)d\theta \qquad (7)$$

In view of the various physiochemical uncertainties about strained flames, not only is Eq (7) computationally convenient but also this concept of S_q is probably sufficiently accurate. Implicit in Eqs (6) and (7) is the independence of flamelet strain rate of time. As suggested earlier, this is probably justifiable.

FLAME STRAIN IN TURBULENT FLOWS

A number of questions emerge in deciding upon the most appropriate strained laminar flame data for turbulent modelling. First, which of the boundary conditions covered in Fig. 4 is more appropriate, or is some other condition to be preferred ? Curvature of the flamelets must be relevant. Second, because in turbulent flow there is no single valued strain rate, what is the pdf for the distributed values ? Third, what is the relationship between aerodynamic strain rates and those acting on the flame ? Here anisotropy can be important.

In non-reacting, turbulent flow Batchelor has shown that for high Reynolds numbers, the

lagrangian mean strain rate of a material surface element of area, A, is

$$\overline{\frac{1}{A}\frac{dA}{dt}} = 0\left(\frac{\varepsilon}{\nu}\right)^{0.5} \tag{8}$$

where ε is the rate of turbulent energy dissipation per unit mass and ν is the kinematic viscosity (ref. 36). For isotropic turbulence (ref. 37)

$$\frac{\varepsilon}{\nu} = 15\left(\frac{u'}{\lambda}\right)^2 \tag{9}$$

In order to quantity the lagrangian pdf of the flame surface strain rate s, p(s), we have assumed that material line elements of the flame surface always tend towards the axis of maximum positive principal strain (ref. 38). When this is so, in isotropic flow, with the eulerian pdfs of the three orthogonal strain rates identical, and with a gaussian distribution, then

$$p(s) = \frac{2}{(2\pi)^{0.5}\sigma}\exp\left(-\frac{s^2}{2\sigma^2}\right) \quad 0 \leq s \leq \infty \tag{10}$$

$$\text{where} \qquad \sigma = \left(\frac{\varepsilon}{12\nu}\right)^{0.5} \quad \text{and} \quad \bar{s} = \left(\frac{\varepsilon}{6\pi\nu}\right)^{0.5} = 0.89\,\frac{u'}{\lambda} \tag{11}$$

The mean flame strain rate, $\bar{s}$, is not so different from the mean eulerian aerodynamic strain rate, u'/λ. Measured eulerian pdfs of strain rates in homogeneous isotropic flows tend to be gaussian except at the tail. An alternative distribution that attempts to allow for this is the log-normal one and the effect of this on flame straining also is discussed in ref. 38.

In an attempt to compare quenching in premixed laminar and turbulent flames, the conditions for partial quenching of the latter were observed experimentally for turbulent explosion flames freely propagating through unburnt gas, with isotropic turbulence, in the regime between K = 0.3 and 1.5, indicated in Fig. 1. Three different propane-air mixtures of equivalence ratios, ϕ, of 0.7, 0.8 and 0.9, were exploded in a fan-stirred bomb, with the fans running at three different fan speeds in each mixture. The flames were observed by high speed schlieren photography and the proportion of the total flame surface area that was supporting combustion, A_r, was estimated from the photographs (ref. 38). This proportion was equated to the probability that the cold gas strain rate into the flame was less than a limiting quenching strain rate, S_q. Thus

$$A_r = \int_0^{S_q} p(s)ds = \text{erf}\left(\frac{S_q}{\sqrt{2}\sigma}\right) = \text{erf}\left(\frac{S_q}{\bar{s}\pi^{0.5}}\right) \tag{12}$$

, as $\sigma = (\pi/2)^{0.5}\bar{s}$ for the quasi-gaussian pdf of Eq (10).

From Eqs (9), (11) and (12)

$$A_r = \text{erf}\left(S_q\,\frac{\lambda}{u'}\left(\frac{2}{5}\right)^{0.5}\right) \tag{13}$$

Values of u'/λ were known from the calibration of the turbulence in the bomb by laser doppler velocimetry and the mean values of S_q, obtained from Eq (13), are shown in Table 1.

Also shown, for the three different equivalence ratios of the same gases, are the experimental premixed laminar flame quenching strain rates, $S_{q\bullet}$, of Law et al in ref. 31 and those computed, S_{qc}, by Strahl et al in ref. 34. In both of these cases the flames were of the symmetric counterflow type and the quenching strain rate, not surprisingly, increases with equivalence ratio. The turbulent bomb values of S_q are about six times those in the laminar flame and about three times those computed. One partial explanation for these differences is that in the turbulent bomb some hot gas was always present to act as a re-ignition source and, consequently, these higher quenching strain rates should, more realistically, be compared with those in asymmetric laminar counterflow, in which one stream is of hot gas. Shown in Fig. 4, in addition to the computed profiles of maximum heat release rate against strain rate for the two laminar, counterflow, conditions for a methane-air flame, is a strain rate marked "1". This corresponds to

that which might be expected for turbulent flame quenching in the stirred bomb. The symmetric condition suggests the flame should quench at a much lower strain rate, whilst the asymmetric condition suggests the flame should never extinguish.

The high experimental value of quench strain rate would be reduced to about 0.7 of the value if, instead of assuming material surfaces into the flame align with the plane of maximum strain rate, it were assumed that they align with the maximum of any three randomly selected positive strain rates. Such a strain rate is marked "2" in the figure. Pope has suggested that, for material surface elements, there is a 30% probability of negative strain rates (ref. 39). This might reduce the observed quenching strain rate to about 0.6 of the initial value, indicated by point "3". A recent direct numerical simulation of isothermal, homogeneous, turbulence has shown the total rate of strain of a material surface to be extensively positive, with an 80% probability (ref. 40).

It is possible that the actual volumetric heat release rate - strain rate profiles in flamelets are intermediate between the symmetric and asymmetric profiles, as a consequence of variable hot boundary conditions and flame curvature. Such a possible intermediate profile is shown dotted in Fig. 4. In this respect, computations for the asymmetric case, but with different values of hot boundary temperature, would be informative.

TABLE 1. Flame-quenching strain rates for propane-air mixtures under different conditions.

ϕ	Fan Speed (r.p.m.)	u'/λ (s^{-1})	S_q (s^{-1})	$S_{q\bullet}$ (s^{-1})	S_{qc} (s^{-1})	K_f/K	K
0.7	3000	2250	2160	340	770	0.32	0.44
	4000	3410	2390			0.29	0.67
	4500	4030	2640			0.26	0.79
0.8	6000	5920	5430	820	1320	0.22	0.92
	7000	7660	3800			0.31	1.19
	8000	9150	4410			0.27	1.41
0.9	9000	11170	7420	1300	2120	0.25	0.89
	9500	12130	7610			0.25	0.97
	10000	13140	6650			0.28	1.05

The discrepancy between values of S_q obtained in the turbulent explosions and the laminar flames seems to be greater than can be accounted for by flame curvature or uncertainties as to the form of the strain rate pdf. Because a probable explanation is that the flame material surfaces are not fully aligned with the plane of maximum strain rate, the experimental bomb results might be re-examined on the assumption that the numerical value of the quenching strain rate is, indeed, the same as that computed for the corresponding symmetric laminar flame. The experiments can then reveal the strain rate to which the turbulent flame must have been subjected.

Equation (12) shows how the measured values of A_r yield the ratio $S_q/\bar{s}$. If the strain rates to which the flame is exposed are different from those assumed, but the form of the pdf is still that of the quasi-gaussian, Eq (10), then this ratio is also equal to $S_{qc}/\bar{s}_f$. Here S_{qc} is the quenching strain rate assumed to be that computed for the laminar flame and $\bar{s}_f$ is the mean strain rate acting on the turbulent flamelets. Hence

$$\frac{\bar{s}_f}{\bar{s}} = \frac{S_{qc}}{S_q} \tag{14}$$

These terms can be normalised by δ_l/u_l to give the ratio of the effective flame straining Karlovitz number, K_f, to the eulerian strain Karlovitz number. By invoking Eq (11)

$$\frac{K_f}{K} = \frac{.89\ S_{qc}}{S_q} \tag{15}$$

Values are shown in the penultimate column of Table 1. The ratio has a mean value of 0.27, with a tendency for it to fall slightly with increase in K. This suggests the effective lagrangian turbulent strain rate that affects the flame is about a quarter of the eulerian strain rate, u'/λ, and that negative flame straining rates, about which little is known, are possible. Clearly, more research is needed on this important question and also upon anisotropic effects, that might be expressed by Reynolds stress modelling.

APPLICATION OF FLAMELET MODEL IN RECIRCULATING FLOW

For experimental and computational studies the axially symmetric, jet-stirred, conical ceramic reactor, shown in Fig. 6, was employed. The half angle of the cone was 29°, the radius to the end spherical segment 81 mm, the inlet nozzle diameter 9.5 mm, outer diameter 19 mm and the exit hole in the reactor was 30 mm diameter. Dried premixture of gaseous fuel and air at atmospheric pressure and 288 K entered as a central jet and burnt gases left through the annulus. The first two moment transport equations of Θ, together with the k-ε model for the solution of flow field, were solved numerically. Additional terms have been added to the original k-ε model to account for variable density effects. Favre, mass weighted, averaging (ref. 41) was adopted to simplify correlations involving fluctuating density in conventional time averages. Full details of the models and computations are given in ref. 23.

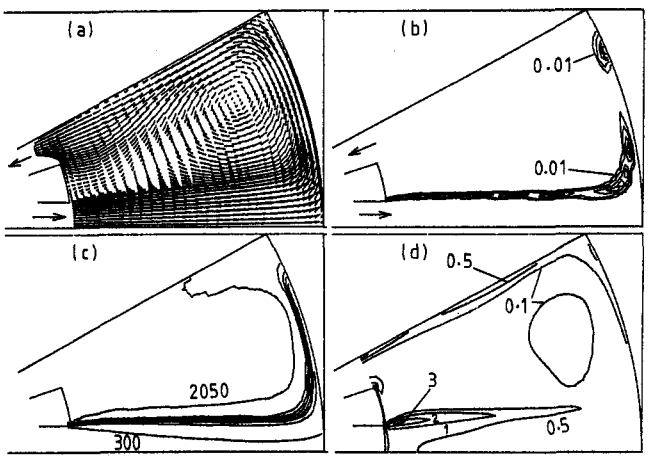

Fig. 6. Methane - air, $\phi = 0.84$, computer contours in jet - stirred, axisymmetric, conical reactor.

(a) Velocity vectors.

(b) $\tilde{q}_t/q_{1max}$ = 0.01 at outer boundaries and 0.5 internal peak. Other values 0.05, 0.1 and 0.3.

(c) T, 300 to 2050 K, increments of 250K.

(d) K.

Figure 6 presents computed results for a premixture of methane-air, equivalence ratio 0.84, and inlet mean velocity 30 m s^{-1}. The value of K based upon the mean velocity at the inlet nozzle is 0.2. The general flow pattern, shown in Fig. 6(a), reveals a large recirculation zone which stabilizes the flame by convecting hot combustion gases to the jet shear layer, where high turbulence is generated to enhance mixing of burning and cold gases. The jet convects the mixing gases downstream as the chemical processes develop. The normalised mean turbulent heat release rate contours in Fig. 6(b), show a maximum value close to where the jet shear layer is deflected and near the top corner. The high jet velocity spreads the flame over the curved wall, as shown by the temperature field in Fig. 6(c). From the computed values of ε/ν, values of Karlovitz stretch factor were calculated from values of u'/λ given by Eq (9) and contours are shown in Fig. 6(d). Within the flame brush, values of K range between 0.1 and 0.5. As pointed out earlier, flame can exist in anisotropic flow fields at the lower values of K and, of course, even at the higher values where a flame cannot exist, non-flame chemical reaction can continue at high temperature.

For such conditions flame straining effects are not severe and ref. 23 reports how gas analyses and temperature measurements at different points in the reactor have validated

this flamelet model. However, as flame straining increases with higher initial values of the product of K and Lewis number at inlet, its effects must be modelled. This is illustrated by some computational results for propane-air mixtures, also studied experimentally and computationally in ref. 23.

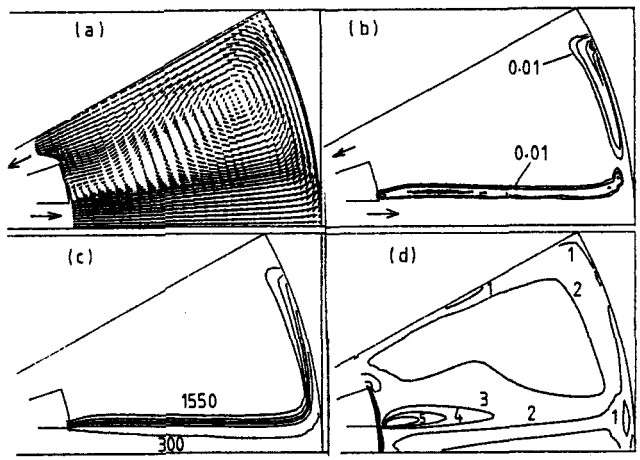

Fig. 7. Propane - air, ϕ = 0.60, computed contours, no allowance for strain.

(a) Velocity vectors

(b) $\bar{q}_t/q_{1max}$ = 0.01 at outer boundaries and 0.5 internal peak. Other values 0.05, 0.1 and 0.3.

(c) T 300 to 1550 K, increments of 250 K.

(d) K.

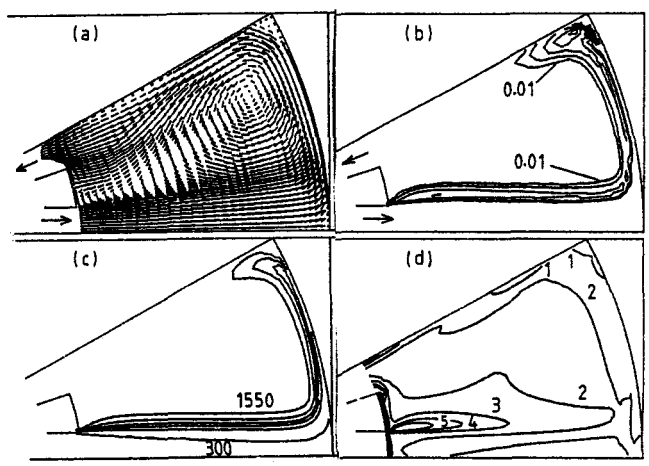

Fig. 8. Conditions as for Fig. 7, but with allowance for strain. Note the extension of the heat release zone in (b) and broadening of the isotherms in (c).

Figures 7 and 8 show different computed profiles for a propane-air equivalence ratio of 0.60, and an inlet mean velocity of 30 m s^{-1}. For this mixture the value of q_{1max} is 2 GW m^{-3}. Flame straining effects are greater than for the methane-air conditions of Fig. 5, on account of the higher initial values of both K (0.85) and Lewis number. The propane oxidation kinetics are described in ref. 23. Allowance for the quenching effects of flame straining now is based on the experimental findings of the previous section. The flame strain integral for $\bar{q}_t$ in Eq (7) is evaluated by Eq (12). In this, S_q is an estimated laminar strain flame computed value, of 500 s^{-1}, and $\bar{s}$ is a mean flame strain rate, given by 0.27 u'/λ.

Figure 7 shows contours without any allowance for strain and Fig. 8 shows these when such an allowance is made in the flamelet model. Figures 7(a) and 8(a) show the allowance to make but little difference to the flow pattern. Not surprisingly, Figs. 7(b) and 8(b) show important differences in the normalised mean turbulent heat release rate. Allowance for quenching extends and thickens the reaction zone, also revealed by the isotherms in Figs. 7(c) and 8(c). This was confirmed by experimental measurements. Localised values of K, in Figs. 7(d) and 8(d), are shown to be high enough to give significant changes in the heat release and temperature contours.

CONCLUSIONS

Initial application of a library of strained, premixed laminar flame data to the mathematical modelling of turbulent combustion has been promising. In particular, the value of heat release rate - reactedness profiles has been demonstrated. Experiments show good predictive ability that declines with increasing strain rates. Similar computational and experimental laminar flame data should be obtained for other fuel - air mixtures, to extend further the practical applications of such modelling. This is also relevant to so - called diffusion flames, in so far as there is always premixing before combustion.

The accuracy of the predictions will improve with further elucidation of the relationships between laminar and turbulent flame strain and aerodynamic strain. More also needs to be known about the pdfs of turbulent flame temperatures and strain rates. Lasers offer attractive, non - intrusive techniques, but there are problems in obtaining meaningful measurements with the requisite spatial and temporal resolutions.

REFERENCES

1. D. Bradley, Proceedings of Workshop on Gas Flame Structure : Part I, p.15, USSR Academy of Sciences, Novosibirsk (1984).
2. R. Borghi, in Recent Advances in Aerospace Sciences, Plenum Press, New York (1985).
3. R.G. Abdel-Gayed, D. Bradley and F.K.K. Lung, Combust. Flame 76, 213-218 (1989).
4. R.G. Abdel-Gayed, K.J. Al-Khishali and D. Bradley, Proc. Roy. Soc. (London) A391, 393-414 (1984).
5. R.G. Abdel-Gayed and D. Bradley, Combust Flame 62, 61-68 (1985).
6. R.G. Abdel-Gayed and D. Bradley, Phil. Trans. Roy. Soc. (London) A301, 1-25 (1981).
7. F. Williams, Combust. Flame 26, 269-270 (1976).
8. B.E. Launder and D.B. Spalding, Comput. Meths. Appl. Mech. Engrg. 3, 269-289 (1974).
9. B.E. Launder, G.J. Reece and W. Rodi, J. Fluid Mech. 68, 537 (1975).
10. D. Bradley, S.B. Chin, P.H. Gaskell, A.K.C. Lau and M. Missaghi, International Conference on Computers in Engine Technology, p.315, Institution Mechanical Engineers, London (1987).
11. P.H. Gaskell and A.K.C. Lau, Fifth (International) Conference on Numerical Methods in Laminar and Turbulent Flow, p.351, (1987).
12. P.H. Gaskell and A.K.C. Lau, Proc. First National Fluid Dynamic Congress AIAA 88-3652, p.272, (1988).
13. W.A. Abd Al-Masseeh, D. Bradley, P.H. Gaskell and A.K.C. Lau, Seventh Turbulent Shear Flow Symposium, Stanford, to be published (1989).
14. W.P. Jones, in Prediction Methods for Turbulent Flow, p. 379, Hemisphere, Washington (1980).
15. K.N.C. Bray, P.A. Libby and J.B. Moss, Combust. Flame 61, 87-102 (1985).
16. P.A. Libby and K.N.C. Bray, AIAA J. 19, 205 (1981).
17. P.H. Gaskell and A.K.C. Lau, Combust. Flame 73, 215-220 (1988).
18. B.P. Leonard, Comput. Meths. Appl. Mech. and Engrg. 19, 59-98 (1979).
19. D. Bradley, M. Missaghi and S.B. Chin, Comput. Meths. Appl. Mech. Engrg. 69, 133-151 (1988).
20. P.H. Gaskell and A.K.C. Lau, Int. J. Num. Meth. Fluids 8, 617-641 (1988).
21. A.Y. Abdalla, D. Bradley, S.B. Chin and C. Lam, Oxidation Communications 4, 113-130 (1983).
22. K.N.C. Bray, Seventeenth Symposium (International) on Combustion, p. 223, Combustion Institute, Pittsburgh (1979).
23. D. Bradley, L.K. Kwa, A.K.C. Lau, M. Missaghi and S.B. Chin, Combust. Flame 71, 109-122 (1988).
24. K.N.C. Bray, P.A. Libby and J.B. Moss, Combust. Flame 61, 87-102 (1985).
25. K.N.C. Bray, M. Champion and P.A. Libby, Combust. Sci. Tech. 59, 463-469 (1988).
26. K.N.C. Bray, M. Champion and P.A. Libby, Twenty-second Symposium (International) on Combustion, p. 763, Combustion Institute, Pittsburgh, (1989).
27. G. Dixon-Lewis and S.M. Islam, Nineteenth Symposium (International) on Combustion, p.283, Combustion Institute, Pittsburgh (1982).
28. R.J. Lewis and J.B. Moss, Seventeenth Symposium (International) on Combustion, p. 267, Combustion Institute, Pittsburgh (1979).
29. A.M. Klimov, Zh. Prikl. Mekh. Tekhn. Fiz. 3, 49-58 (1963).
30. H. Tsuji and I. Yamaoka, First Specialists Meeting (International) of the Combustion Institute : Tome I, p. 111, Section Francaise du Combustion Institute (1981).
31. C.K. Law, D.L. Zhu and G. Yu, Twenty-first Symposium (International) on Combustion, p. 1419, Combustion Institute, Pittsburgh (1988).
32. F.A. Williams, Combustion Theory, Second Edition, Benjamin/Cummings, Menlo Park (1985).

33. G. Dixon-Lewis, Proceedings of Workshop on Gas Flame Structure : Part 2, p. 3, USSR Academy of Sciences, Novosibirsk (1988).
34. G. Strahl, B. Rogg and J. Warnatz, Dynamics of Reactive Systems Part 1 : Flames, Vol. 113 Progress in Astronautics and Aeronautics, p. 195, AIAA, Washington (1988).
35. G. Dixon-Lewis, Dynamics of Reactive Systems Part 1 : Flames, Vol. 113 Progress in Astronautics and Aeronautics, p. 166, AIAA, Washington (1988).
36. G.K. Batchelor, Proc. Roy. Soc. (London) A213, 349-366 (1952).
37. G.I. Taylor, Proc. Roy. Soc. (London) A151, 421-444 (1935).
38. R.G. Abdel-Gayed, D. Bradley and A.K.C. Lau, Twenty-second Symposium (International) on Combustion, p. 731, Combustion Institute, Pittsburgh (1989).
39. S.B. Pope, Twenty-second Symposium (International) on Combustion, discussion of ref. 38, p. 738, Combustion Institute, Pittsburgh (1989).
40. P.K. Yeung, S.S. Girimaji and S.B. Pope, Straining and scalar dissipation on material surfaces in turbulence : implications for turbulence, Report FDA-88-23, Sibley School of Mechanical and Aerospace Engineering, Cornell University (1988).
41. R.W. Bilger, Combust. Sci. Tech. 11, 215-217 (1975).